Journal of Fluids Engineering

Technical Briefs

On End-Wall Corner Vortices in a Lid-Driven Cavity

T. P. Chiang,[1] Robert R. Hwang,[1] and W. H. Sheu[1]

We conducted a flow simulation to study the laminar flow in a three-dimensional rectangular cavity. The ratio of cavity depth to width is 1:1, and the span to width aspect ratio (SAR) is 3:1. The governing equations defined on staggered grids were solved in a transient context by using a finite volume method, in conjunction with a segregated solution algorithm. Of the most apparent manifestation of three-dimensional characteristics, we addressed in this study the formation of corner vortices and its role in aiding the transport of fluid flows in the primary eddy and the secondary eddies.

1 Introduction

Recirculating flow is commonplace in many engineering fields. Conducting analyses to gain insight into the evolution of vortical flows is, thus, critical for developmental engineers. We considered in this study an extensively studied lid-driven flow in a rectangular cavity with the depth to width ratio, 1:1, and the span to width ratio, 3:1 (see Fig. 1). Geometric simplicity of this problem facilitates both experimental calibrations and numerical predictions.

Experimentally, the lid-driven cavity problem was first investigated by Pan and Acrivos (1967), followed by numerous visualization studies (Koseff and Street, 1984; Aidun et al., 1991). These measurement data suffice to depict a salient flow pattern. The pioneer numerical work was due to Burggraf (1966), who conducted only two-dimensional analysis. With the advent of high-speed computers and ever-increasing large disk space, three-dimensional simulations (Freitas et al., 1985; Ku et al., 1987; Freitas and Street, 1988; Cortes and Miller, 1994) have become feasible and are a great aid in acquiring additional details. Notable, among others, is the numerical confirmation of the laboratory observed corner vortices (Koseff et al., 1983).

From knowledge gained from the previous studies, it is now a generally recognized fact that the cavity of interest is filled with a primary eddy, downstream and upstream secondary eddies, and possibly meandering Taylor-Görtler longitudinal vortices as the Reynolds number is sufficiently high (see Fig. 1(a)). Previous investigations, however, did not focus much on the end-wall corner vortices other than noting their existence. This motivated us to conduct the present study with an aim to improve our understanding of corner vortices present near the end wall of the lid-driven cavity.

2 Governing Equations and Numerical Procedures

We considered in this study the following dimensionless velocity-pressure formulation for an incompressible Navier-Stokes fluid flow:

$$\frac{\partial u_i}{\partial x_i} = 0, \tag{1}$$

$$\frac{\partial u_i}{\partial t} + \frac{\partial}{\partial x_m}(u_m u_i) = -\frac{\partial p}{\partial x_i} + \frac{1}{\mathrm{Re}}\frac{\partial^2 u_i}{\partial x_m \partial x_m}, \tag{2}$$

where $i = 1 \sim 3$. Hereinafter, we denote u_i and p as the velocity components and the modified pressure, respectively. In Eq. (2), $\mathrm{Re} = (U_c B/\nu)$ is referred to as the Reynolds number, where ν stands for the kinematic viscosity, B the width of the cavity, and U_c the lid velocity.

To avoid oscillatory solutions in the pressure field, the present analysis is formulated for staggered grids (Patankar, 1980). Use of grid staggering demands velocity nodes to be stored only at the control faces. This grid arrangement facilitates conducting a finite volume integration of working equations in their representative control volume. In modeling the equations of motion, a higher-order QUICK scheme of Leonard (1979) has been the choice for discretizating the non-linear advective fluxes. Among the possible solution algorithms to solve for primitive variables, we adopted the segregated approach, known as the SIMPLE (Patankar, 1980) solution algorithm. The readers are referred to the work of Patankar (1980) for additional details.

3 Code Validation

Prior to predicting the flow physics in the rectangular cavity, we conducted a validation study by solving a problem which is amenable to analytic Navier-Stokes solutions. In a cubical cavity of unit length, we carried out the analysis on a $31 \times 31 \times 31$ uniform grid system. Subject to the boundary velocities given by $(u, v, w) = (\frac{1}{2}(y^2 + z^2), -z, y)$ the exact pressure solution takes the following form:

$$p = \tfrac{1}{2}(y^2 + z^2) + \frac{2}{\mathrm{Re}}x.$$

According to the computed errors cast in an L_2-norm form for primitive variables, namely (0.55×10^{-6}, 0.19×10^{-6}, 0.13

[1] Associate Professor, Professor, and Professor, respectively, Department of Naval Architecture and Ocean Engineering, National Taiwan University, 73 Chou-Shan Rd., Taipei, Taiwan.

Contributed by the Fluids Engineering Division of THE AMERICAN SOCIETY OF MECHANICAL ENGINEERS. Manuscript received by the Fluids Engineering Division May 24, 1996; revised manuscript received September 18, 1996. Associate Technical Editor: S. A. Jordan.

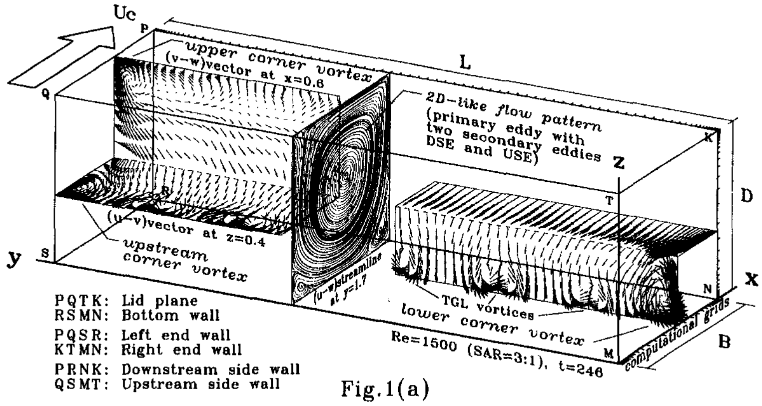

Fig.1(a)

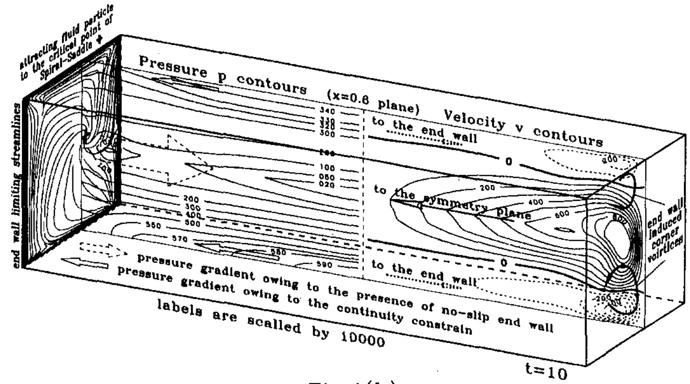

Fig.1(b)

Fig. 1 Problem definition and the description of the end wall effects. (*a*) Global flow structure; (*b*) the end wall induced pressure contours and spanwise velocity contours.

$\times 10^{-6}$, 0.23×10^{-4}) for (u, v, w, p) respectively, together with the maximum relative errors, (0.1×10^{-2}, 0.11×10^{-4}, 0.12×10^{-4}, 0.12×10^{-2}), we confirmed the validity of the proposed discretization method.

Having successfully completed an analytic validation test, we conducted also a grid refinement test for further confirmation of the computer code being developed. The target problem was that of the lid-driven cavity problem of the present interest. Here, we considered Re = 1000 and spanwise aspect ratio SAR = 1:1 for comparison purposes. With good agreement with other predicted velocities u ($x = 0.5$, $y = 0.5$, z) and w (x, $y = 0.5$, $z = 0.5$), as shown in Fig. 2, and the success of grid refinement test, it is concluded that the proposed analysis tool is well-suited for solving incompressible Navier-Stokes equations.

4 Results and Discussions

In Fig. 1(a), the configuration of the present interest is defined by two ratios, namely, depth to width (D/B = 1:1) and span to width (L/B = 3:1). In this study the mesh, with a grid of resolution of $34 \times 91 \times 34$, was stretched in regions where the boundary layers may develop. For this study, we considered Re = 1500. The emphasis was placed on the formation of the corner vortices, as shown in Fig. 1(a), in the vortical flow development.

4.1 End Wall Effect. A manifestation of this three-dimensional flow is the spanwise component generated by the two end walls. As shown in Fig. 1(b), the decelerating fluid particles adjacent to the end walls induce a negative pressure gradient. This, in turn, causes an inward spanwise flow motion inside the primary cell. Under these circumstances, a positive spanwise pressure gradient in the regions near the lid plane and the floor of the cavity is established. Mass continuity demands that the particles proceed toward the two end-walls. This conceptually amounts to placing a suction pump in the core region so that the fluid particles near the junctures of the floor, lid plane, and the upstream and downstream side walls of the cavity are entrained to both end-walls. It is also important to note that a less apparent outward-running spiral motion is visible near the lid plane. These spiraling particles will be finally engulfed into the primary core via corner vortices present near the two end walls.

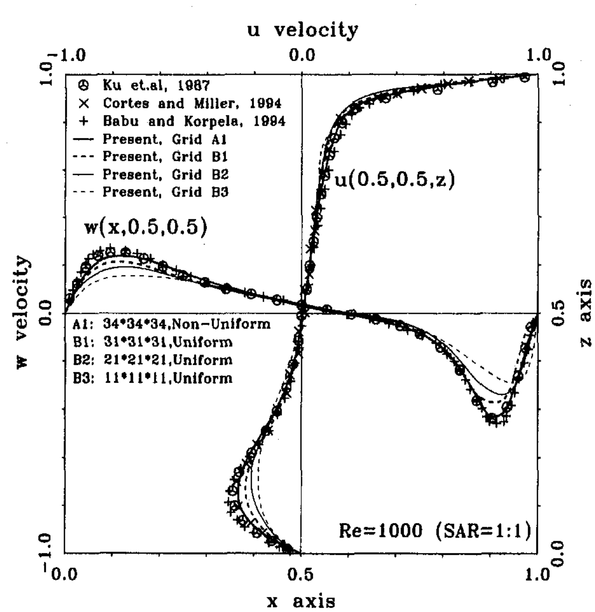

Fig. 2 Comparison studies with other numerical solutions for velocity profiles $u(0.5, 0, 5, z)$ and $w(x, 0.5, 0.5)$, together the grid convergence test for Re = 1000

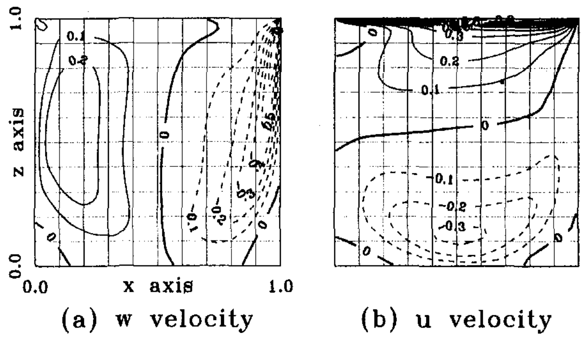

Fig. 3 The velocity contours at the $y = 2.0$ plane at $t = 24$. (*a*) *w* velocity; (*b*) *u* velocity

4.2 x-Plane Corner Vortices. The end-wall corner vortices are not necessarily present at the upper and lower corners of the x planes. Their presence is rather dependent on the spanwise and the primary circulating flow motions. As indicated in Fig. 3(a), in the upper cavity fluid particles which are characterized as possessing $w > 0$, as a direct result of the character of primary flow, can facilitate the formation of the upper corner vortices. On the other hand, the downward velocity $w < 0$ aids in forming a lower corner vortex. According to Fig. 4(a), lower corner vortices under no circumstances can be found in regions of $x < 0.5$, where $w > 0$. As the $x = 0.7$ plane is approached, descending fluids, as shown in Fig. 4(b), cause the upper corner vortex to disappear. Whether or not corner vortices at x planes will be finally established depends on the sign of the w velocity component in the primary vortex motion (see Fig. 3). Simply stated, $w > 0$ in the upper cavity while $w < 0$ in the lower cavity allow the formation of corner vortices at every account.

Corner eddies are believed to be the result of a mutual adjustment of the shear and the pressure forces to the no-slip condition applied at the two end walls. These stress-induced vortices cause a rotational flow (see Fig. 5). Vortices of this kind are prone to depart from the two end walls and aid the nearby particles being engulfed into the primary flow. Also notable is that the centroids of corner vortices are not necessarily close to the corner. Once the upper corner vortex forms, it is situated at the corner. In contrast, the center of the lower corner vortex is comparatively distant away from the intersection of the floor and the two end walls. This phenomenon is shown at the $x = 0.8$ plane in Fig. 6. To provide us with useful guidance for examining whether or not these corner vortices will form, we have plotted contour lines of $w = 0$ and $v = 0$ in Figs. 4–6. So long as a line of $w = 0$ intersects the line of $v = 0$, corner vortices are expected to form.

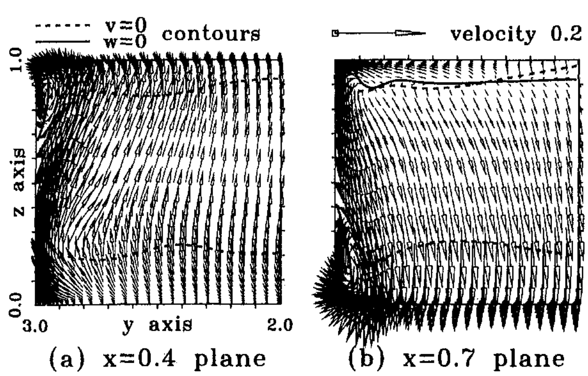

Fig. 4 Flow structures at two x planes at $t = 24$. (*a*) $x = 0.4$ plane; (*b*) $x = 0.7$ plane.

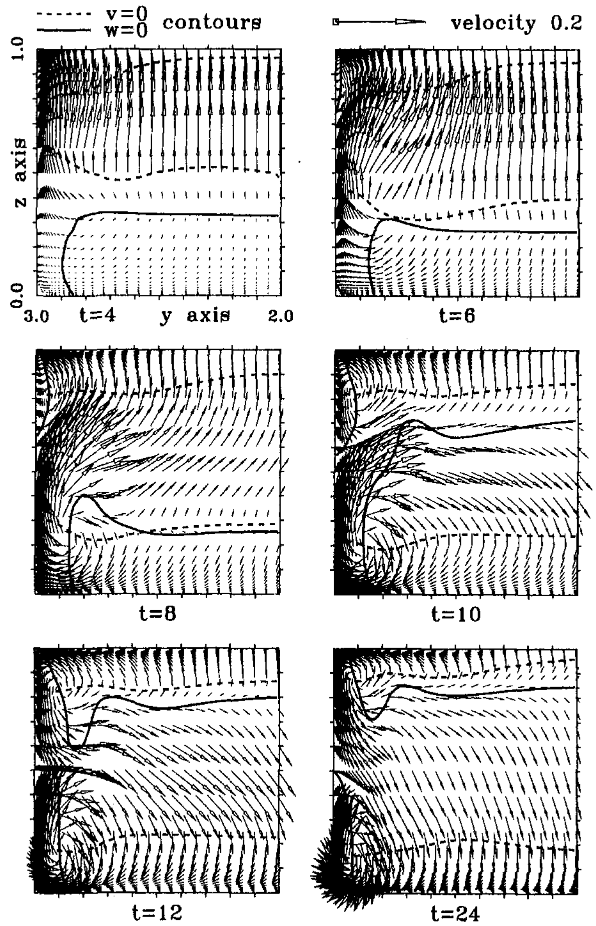

Fig. 5 Development of corner vortices at the $x = 0.6$ plane at $t = 4$, 6, 8, 10, 12, and 24

4.3 z-Plane Corner Vortices. In the z-plane, flow patterns in Fig. 7 bear strong resemblance to those computed at the x planes. Like the streamwise location of x plotted in Fig. 3(a) for which $w = 0$, the location of z that demands $u = 0$ in

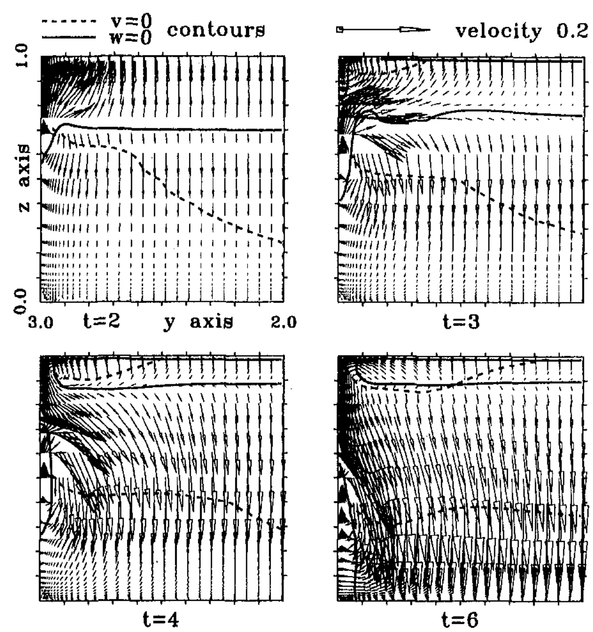

Fig. 6 Flow structures at the $x = 0.8$ plane at $t = 2$, 3, 4, and 6

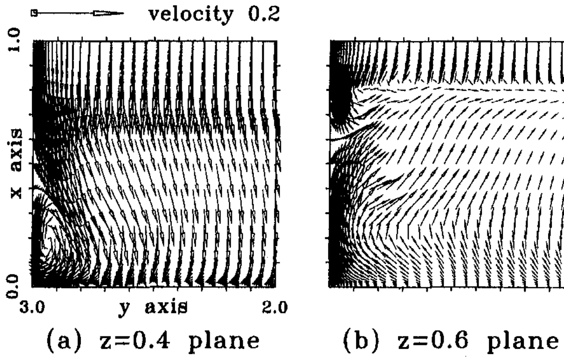

Fig. 7 Flow structure at two z planes at t = 24. (a) at z = 0.4 plane; (b) at z = 0.6 plane

Fig. 3(b) plays an essential role in judging whether the upstream corner vortex can be formed at the z planes. In Fig. 3(b), zero contour profiles of $u = 0$ closely resemble those of $w = 0$ in Fig. 3(a), except in the region fairly near the lid plane where $w = 0$ and $u = 1$. In view of the degree of physical complications, flow patterns at different z planes are regarded as much simpler than those at x planes. Unlike the upper and lower corner vortices at the x planes, the downstream corner vortices are hardly visible at the z planes. Except at the lid plane where $u = 1$, the value of u is less than zero in regions close to $x = 1$. Such a negative velocity gives rise to a strongly rotational downstream corner eddy in regions fairly close to $z = 1$.

4.4 The Role of Corner Vortices. As Fig. 1(a) reveals, there exist corner vortices in the cavity. The formation of such corner vortices constitutes the global transport structure in that fluid particles near the two end walls are engulfed into the primary core with the aid of corner vortices. Corner vortices, as a consequence, aid the exchange of fluid flows in the cavity. Conceptually, this amounts to placing a suction pump near the end wall, to which the nearby particles are attracted. In support of this statement, we plotted in Fig. 8 the particle tracers. Particles are clearly sucked into the attracting spiral saddle point via the corner vortices.

5 Conclusions

In the present analysis, we considered the incompressible fluid flow inside the investigated 3:1:1 cavity. Of three dimensional spiraling features, we have addressed under what conditions corner vortices will form. Through this study, it is concluded that the presence of corner vortices in the vicinity of two end-walls aids flow transport. Fluid particles coming across corner vortices will be lifted up and then drawn in the spiral-saddle point and then spiral towards the symmetry plane in the primary core.

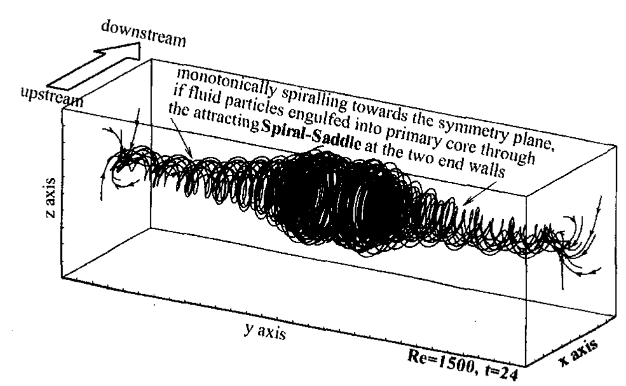

Fig. 8 Particle tracers for illustration of the attraction of fluids to the saddle point with the aid of corner vortices

Acknowledgment

The authors would like to express their thanks for financial support from the National Science Council under contract number NSC 80-0410-E002-51.

References

Aidun, C. K., Triantafillopoulos, N. G., and Benson, J. D., 1991, "Global Stability of a Lid-Driven Cavity with Throughflow: Flow Visualization Studies," *Phys. Fluids*, Vol. A3, pp. 2081–2091.

Babu, V. and Korpela, S. A., 1994, "Numerical Solutions of the Incompressible, Three-Dimensional Navier-Stokes Equations," *Computer Fluids*, Vol. 23, No. 5, pp. 675–691.

Burggraf, O. R., 1966, "Analytical and Numerical Studies of the Structure of Steady Separated Flows," *Journal of Fluid Mechanics*, Vol. 24, No. 1, pp. 113–151.

Cortes, A. B., and Miller, J. D., 1994, "Numerical Experiments With the Lid-Driven Cavity Flow Problem," *Computer Fluids*, Vol. 23, No. 8, pp. 1005–1027.

Freitas, C. J., Street, R. L., Findikakis, A. N., and Koseff, J. R., 1985, "Numerical Simulation of Three-Dimensional Flow in a Cavity," *Int. J. Numer. Methods Fluids*, Vol. 5, pp. 561–575.

Freitas, C. J., and Street, R. L., 1988, "Non-Linear Transport Phenomena in a Complex Recirculating Flow: A Numerical Investigation," *Int. J. Numer. Meths. in Fluids*, Vol. 8, pp. 769–802.

Koseff, C. J., Street, R. L., Gresho, C. D., Upson, J. A., Humphrey, J. A. C., and To, W. H., 1983, "A Three-Dimensional Lid-Driven Cavity Flow: Experiment and Simulation," *Proc. 3rd Int. Conf. Num. Meth. Lam. and Turb. Flow, Seattle*, Aug.

Koseff, J. R., and Street, R. L., 1984a, "Visualization Studies of a Shear Driven Three-Dimensional Recirculating Flow," ASME Journal of Fluids Engineering, Vol. 106, No. 1, pp. 21–29.

Koseff, J. R. and Street, R. L., 1984b, "On End Wall Effects in a Lid-Driven Cavity Flow," ASME Journal of Fluids Engineering, Vol. 106, pp. 385–389.

Koseff, J. R. and Street, R. L., 1984c, "The Lid-Driven Cavity Flow: A Synthesis of Qualitative and Quantitative Observations," ASME Journal of Fluids Engineering, Vol. 106, pp. 390–398.

Ku, H. C., Hirsh, R. S., and Taylor, T. D., 1987, "A Pseudospectral Method for Solution of the Three-Dimensional Incompressible Navier-Stokes Equations," *J. Comput. Phys.*, Vol. 70, pp. 439–462.

Leonard, B. P., 1979, "A Stable and Accurate Convective Modeling Procedure Based on Quadratic Upstream Interpolation," *Comput. Methods Appl. Mech. Engrg.*, Vol. 19, pp. 59–98.

Pan, F., and Acrivos, A., 1967, "Steady Flows in Rectangular Cavities," *Journal of Fluid Mechanics*, Vol. 28, pp. 643–655.

Patankar, S. V., 1980, *Numerical Heat Transfer and Fluid Flow*, Hemisphere.

Effects of N^+ Ion Implantation on Surface Modification of Cavitation Damage for 0Cr13Ni9Ti SS of Turbine Materials

Jian Hua Wu and Gong Chun Chai

In this paper, six technologies have been used to implant N^+ into 0Cr13Ni9Ti SS, which is a kind of general turbine material in China, and their comparative experiments have been done to get a much better technology of modification of cavitation damage. The results show that the ability of cavitation resistance for 0Cr13Ni9Ti SS by N^+ ion implantation can reach

[1] Senior Engineer and Professor, Senior Engineer, respectively, Nanjing Hydraulic Research Institute, 225 Guangzhou Road, Nanjing, 210029, People's Republic of China.

Contributed by the Fluids Engineering Division of The American Society of Mechanical Engineers. Manuscript received by the Fluids Engineering Division August 31, 1995; revised manuscript received August 12, 1996. Associate Technical Editor: J. Katz.